


RAPID COMMUNICATION

Identification of cavotricuspid isthmus voltage patterns in typical atrial flutter ablation

Francisco Ribes MD  | Ángel Ferrero-de-Loma-Osorio MD, PhD |
Juan Miguel Sánchez-Gómez MD | Lourdes Bondanza MD | Ángel Martínez-Brotons MD |
Ricardo Ruiz-Granell MD, PhD

Department of Cardiology, Arrhythmia Unit, Hospital Clínico Universitario Valencia, Valencia, Spain

Correspondence

Francisco Ribes, Department of Cardiology, Arrhythmia Unit, Hospital Clínico Universitario Valencia, Av. Blasco Ibáñez, 17, Valencia, Spain.
Email: fribestur@gmail.com

Abstract

Background: Electroanatomical mapping is an essential tool in the ablation of typical AFL.

Objectives: To identify the existence of voltage patterns in the CTI voltage maps and their relevance for typical AFL ablation.

Methods: A voltage map of the CTI was made prior to ablation, identifying the areas of maximum voltage and their location along the CTI, allowing classification into patterns according to their distribution. A stepwise ablation approach targeting the areas of maximum voltage was conducted. The ablation characteristics were compared based on the pattern obtained.

Results: Two voltage patterns were identified, with differences in ablation time to bidirectional CTI block. No complications occurred.

Conclusions: Voltage mapping identifies patterns in the CTI with implications for typical AFL ablation.

KEYWORDS

cavotricuspid isthmus, typical atrial flutter, voltage mapping, voltage patterns radiofrequency ablation

1 | BACKGROUND

Since the early days of cavotricuspid isthmus (CTI) ablation, the usual approach has been to perform a radiofrequency (RF) dotted line in the base of the right atrium (RA), joining the tricuspid annulus (TA) and the inferior vena cava (IVC), with the aid of fluoroscopy.^{1,2} With the generalization of electroanatomical navigation systems, the procedure has become safer, avoiding unwanted complications and virtually eliminating the dose of fluoroscopy administered. However, the anatomical approach, with an RF line between the TA and the IVC edges, is still standard practice. In this work, we aim to analyze the voltage maps of the CTI in order to identify the existence

of repetitive voltage patterns and to determine their usefulness and relevance in atrial flutter ablation (AFL).

2 | METHODS

2.1 | Voltage pattern acquisition

A total of 68 patients with typical AFL, who were referred to our center for CTI ablation, were prospectively enrolled. In all cases, voltage mapping was performed with the *Ensite Navx* navigation system in its *Precision™* version [Abbott, Chicago, IL], using as

This is an open access article under the terms of the [Creative Commons Attribution-NonCommercial-NoDerivs](https://creativecommons.org/licenses/by-nc-nd/4.0/) License, which permits use and distribution in any medium, provided the original work is properly cited, the use is non-commercial and no modifications or adaptations are made.
© 2024 The Authors. *Journal of Arrhythmia* published by John Wiley & Sons Australia, Ltd on behalf of Japanese Heart Rhythm Society.

reference catheter a preformed duodecapolar *Orbiter™* [Boston Scientific Corp, Marlborough, MA] placed in the coronary sinus (CS) and in close contact with the TA. A *TactiCath™* mapping and ablation catheter (3.5 mm-irrigated tip) [Abbott, Chicago, IL] was then used for high-density mapping. Voltage mapping of the CTI was performed either in sinus rhythm (SR) or in AFL, from the TA to the IVC. Previous studies described lower voltages in AFL than in SR or stimulated rhythm. This concern was mitigated by defining de areas of interest as a proportion of the V_{max} .³

2.2 | Voltage pattern identification

After the acquisition of the voltage maps, the maximum voltage (V_{max}) was selected. First zone 1 (Z1) was delimited with voltages between 80 and 100% of V_{max} and zone 2 (Z2) with voltages between 60% and 80% of V_{max} (Figure 1).

We were able to identify two distribution patterns of Z1 and Z2 along the central CTI (Figure 2). Pattern or group 1 (G1) had Z1 in the middle zone of the CTI, while Z2s were limited to the TA and IVC aspects. A second group, group 2 (G2) in which Z1 was not located in

the middle zone of the CTI, but in the areas close to the TA and IVC, whereas Z2 occupied the middle part.

2.3 | Electric potential-guided ablation

In our laboratory, voltage-guided ablation was performed in a step-wise fashion, initiating applications in Z1 and continuing them in Z2 only if bidirectional CTI block was not achieved. The preset power was 40W and the target was to reach an LSI (*Lesion Index™*) ≥ 5 or until the atrial electrogram abatement.⁴ If the patient was in sinus rhythm, applications were performed during pacing from the CS, and the RA lateral wall activation sequence was monitored. Once a change in the sequence was detected, the applications were interrupted, and bidirectional CTI block was then checked by differential pacing. If the patient was referred to AFL, the same procedure was followed with applications in Z1 and subsequently in Z2, if necessary, until the arrhythmia was interrupted. Afterward, the CTI was checked for the bidirectional block. If the block was not achieved, the lesion was completed by connecting the ablated areas with the TA and IVC by means of an RF line.

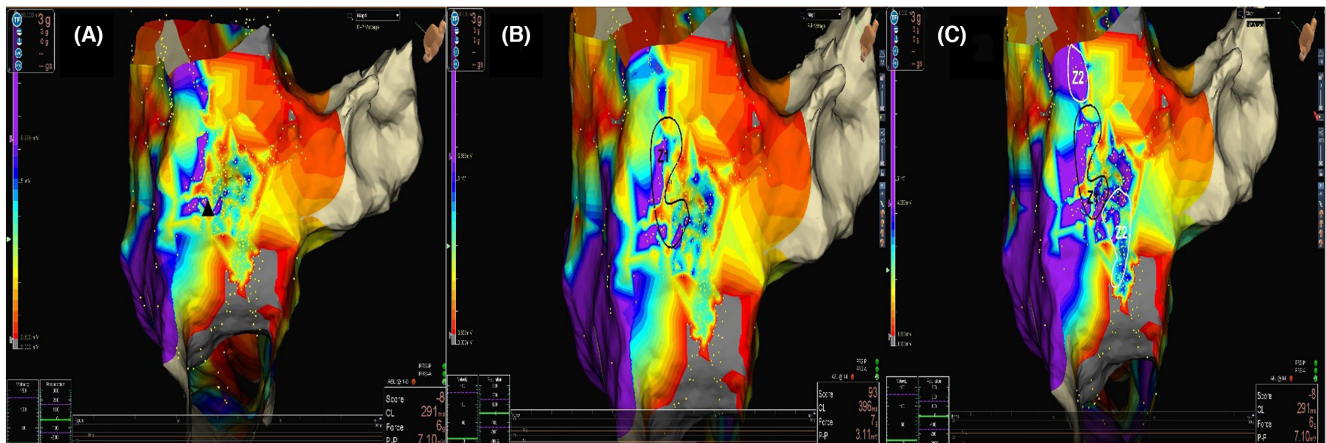


FIGURE 1 CTI voltage mapping. Caudal LAO view. (A) after voltage mapping, V_{max} is selected (black triangle); (B) voltage scale is adjusted to demarcate Z1 ($\geq 80\%$ of V_{max}); (C) voltage scale is again adjusted to define Z2 ($\geq 60\%$ of V_{max}).

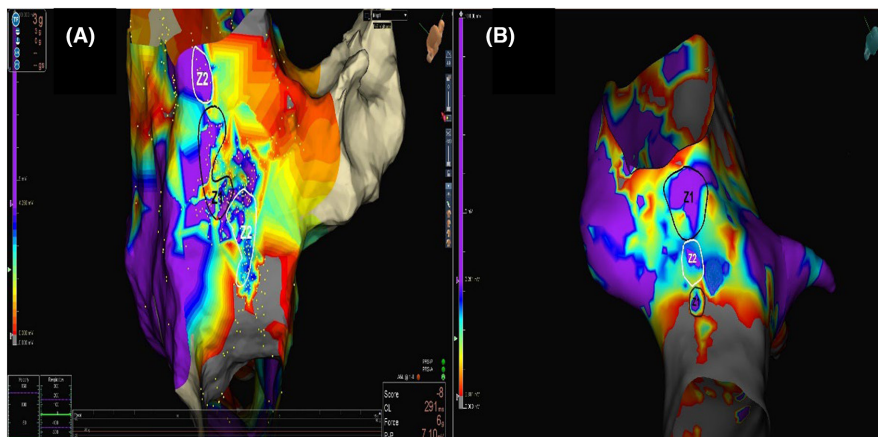


FIGURE 2 CTI voltage patterns according to Z1 and Z2 distribution along the central isthmus. Caudal LAO view. (A) G1 is defined by a Z1 in the middle CTI and Z2s limited to the TA and IVC aspects; (B) G2 is characterized by a Z1 not related to the middle CTI. Instead, Z2 occupies the middle CTI and Z1 areas are located near the IVC and/or TA edges.

TABLE 1 Baseline patient, mapping, and ablation characteristics by group.

	G 1 (n=59)	G 2 (n=9)	p
Baseline characteristics			
Female sex; n (%)	7 (11.9)	3 (33.3)	.09
Age; mean±SD	65±10	63±10	.678
Atrial fibrillation; n (%)	29 (49.2)	7 (77.8)	.109
Hypertension; n (%)	40 (67.8)	4 (44.4)	.172
Diabetes mellitus; n (%)	23 (38.9)	4 (44.4)	.755
Hyperlipidemia; n (%)	32 (54.2)	7 (77.8)	.183
Smoke; n (%)	25 (42.4)	7 (77.8)	.014*
Obstructive sleep apnea	30 (50.8)	4 (44.4)	.72
Heart disease; n (%)			.054
Coronary artery disease	7 (11.9)	1 (11.1)	
Valvular heart disease	5 (8.5)	1 (11.1)	
Nonischemic cardiomyopathy	2 (3.4)	0 (0)	
Tachycardia-induced cardiomyopathy	1 (1.7)	0 (0)	
Hypertensive heart disease	4 (6.8)	1 (11.1)	
LVEF; (%); mean±SD	60±7	52±13	.07*
Atrial enlargement; (>34 mL/m ²); n (%)	31 (52.5)	7 (77.8)	.156
Beta-blockers intake; n (%)	43 (72.9)	4 (44.4)	.085
Antiarrhythmic drugs; n (%)	39 (66.1)	8 (88.9)	.643
Oral antithrombotic agents; n (%)			.353
VKAs	21 (35.6)	2 (22.2)	
NOACs	32 (54.2)	7 (77.8)	
Mapping			
CTI length (mm); mean±SD	31±9.6	27±11.2	.233
CTI area (cm ²); mean±SD	9.1±3.8	7.2±5	.29
Area of interest (cm ²); mean±SD	3.2±2	2.4±1.4	.29
Area of interest/CTI area; mean±SD	0.36±0.19	0.4±0.27	.148
Area of interest average amplitude (mV); mean±SD	4.7±1.5	4±2.2	.249
Average amplitude Z1 (mV); mean±SD	5.4±1.7	4.6±2.5	.219
Average amplitude Z2 (mV); mean±SD	4.2±1.3	3.6±1.9	.48
Total mapped points; mean±SD	313±123	299±170	.827
Mapping rhythm; n (%)			.792
Paced	30 (50.8)	5 (55.6)	
Flutter	29 (49.2)	4 (44.4)	
Mapping time (min); mean±SD	20.5±4.9	22±2.7	.337
Ablation			
Total force (g); mean±SD	10.4±5	13.4±9	.253
Lateral force (g); mean±SD	6.9±2.7	6.5±3.2	.781
Axial force (g); mean±SD	7.2±7.5	10.1±9.6	.428
RF applications; mean±SD	13±7.8	8.1±2.2	.054
RF time per application (s); mean±SD	42.1±21.1	35.5±16.2	.399

TABLE 1 (Continued)

	G 1 (n=59)	G 2 (n=9)	p
RF time (min); mean±SD	8.5±4.4	5.2±2.1	.024*
Ablation required in Z2; n (%)	39 (66.1)	7 (77.8)	.486
Linear lesion; n (%)	3 (5.1)	1 (11.1)	.538
FTI (g/s); mean±SD	399±289	457±291	.67
LSI; mean±SD	5.3±1	5.7±1	.336
Total procedure time (min); mean±SD	68±21	59±18	.333

Abbreviations: CTI, cavostricuspid isthmus; FTI, force-time integral; IQR, interquartile range; LSI, lesion Index; LVEF, left ventricle ejection fraction; NOACs, new oral anticoagulants; RF, radiofrequency; SD, standard deviation; VKAs, vitamin K antagonists; Z1, zone 1; Z2, zone 2. *Statistically significant.

TABLE 2 Correlation of radiofrequency time and mapping characteristics.

	ρ	p
Mapping		
CTI length	-0.015	.9
CTI area	0.046	.71
Area of interest	0.157	.202
Area of interest/CTI area	0.08	.519
Area of interest average amplitude	0.15	.221
Average amplitude Z1	0.154	.209
Average amplitude Z2	0.188	.124

Abbreviations: CTI, cavostricuspid isthmus; Z1, zone 1; Z2, zone 2; ρ , Pearson correlation coefficient.

3 | RESULTS

Two groups were identified according to the voltage patterns of the CTI (Figure 2), G1 being the most frequent (87%), followed by G2 (13%) (Table 1). The area of interest (CTI area corresponding to Z1 and Z2) with respect to the total CTI area was 30% (22%–51%). Voltage-guided ablation achieved bidirectional CTI block in 94.1% of procedures and ablation in Z1 and Z2 was necessary in 67.6%, with no group differences. No differences in electroanatomical features (CTI length, CTI area, and voltage amplitudes in Z1 or Z2) were found between groups.

As shown in Table 1, differences in the time of RF delivered were found between G1 and G2 (8.5±4.4 vs. 5.2±2.1 min) ($p=.024$).

Furthermore, as we can see in Table 2, these findings were independent of voltage recorded in Z1 and Z2 as well as the relative surface area occupied by these zones with respect to the surface of the central CTI. Overall, no correlation was observed between RF time and the need to ablate in Z2 ($p=.489$).

This observation enables us to affirm that the presence of Z1 in the middle part of the CTI requires more RF time for CTI block. From classical CTI anatomy studies and the maximum voltage ablation technique,^{5,6} we know that the middle CTI consists

of discrete *trabeculae* with preferential conduction separated by pouches and areas of nonexcitable fatty tissue. It is likely that ablation of this anatomically irregular area requires more time than the areas adjacent to the TA and IVC, and therefore the presence of Z1 in the middle CTI makes G1 the group requiring the longest RF time.

4 | CONCLUSIONS

The finding of voltage patterns in the CTI and their relationship to the RF time required to achieve CTI block sheds light on its complex structure. The differences found in RF time according to the observed pattern allow us to hypothesize about the influence of the location of the areas of highest voltage on the increased complexity for CTI ablation. A voltage-guided, stepwise ablation approach is an effective technique and appears to be a more physiological approach to this arrhythmia.

AUTHOR CONTRIBUTIONS

All authors contributed equally to this work.

ACKNOWLEDGMENTS

There was no funding source for this study and given permission to be cited.

CONFLICT OF INTEREST STATEMENT

The authors declare no conflict of interest.

ETHICS STATEMENT

This study was approved by the Hospital Clínico Universitario de Valencia Ethics Committee on January 25, 2018.

PATIENT CONSENT STATEMENT

All patients included in this study provided consent to participate.

ORCID

Francisco Ribes  <https://orcid.org/0000-0003-3894-6179>

REFERENCES

1. Feld GK, Fleck RP, Chen PS, Boyce K, Bahnson TD, Stein JB, et al. Radiofrequency catheter ablation for the treatment of human type I atrial flutter. Identification of the critical zone in the re-entrant circuit by endocardial mapping techniques. *Circulation*. 1992;86:1233–40.
2. Cosio FG, Lopez-Gil M, Goicolea A, Arribas F, Barroso JL. Radiofrequency ablation of the inferior vena cava-tricuspid valve isthmus in common atrial flutter. *Am J Cardiol*. 1993;71:705–9.
3. Rodríguez-Mañero M, Valderrábano M, Baluja A, Kreidieh O, Martínez-Sande JL, García-Seara J, et al. Validating left atrial low voltage areas during atrial fibrillation and atrial flutter using multielectrode automated electroanatomic mapping. *JACC Clin Electrophysiol*. 2018;4(12):1541–52.
4. Boles U, Gul E, Fitzpatrick N, Enriquez A, Conroy J, Ghassemian A, et al. Lesion size index in maximum voltage-guided cavotricuspid ablation for atrial flutter. *J Innov Card Rhythm Manag*. 2017;8:2732–8.
5. Redfearn DP, Skanes AC, Gula LJ, Krahn AD, Yee R, Klein GJ. Cavotricuspid isthmus conduction is dependent on underlying anatomic bundle architecture: observations using a maximum voltage-guided ablation technique. *J Cardiovasc Electrophysiol*. 2006;17(8):832–8.
6. Gula LJ, Redfearn DP, Veenhuizen GD, Krahn AD, Yee R, Klein GJ, et al. Reduction in atrial flutter ablation time by targeting maximum voltage: results of a prospective randomized clinical trial. *J Cardiovasc Electrophysiol*. 2009;20(10):1108–12.

How to cite this article: Ribes F, Ferrero-de-Loma-Osorio Á, Sánchez-Gómez JM, Bondanza L, Martínez-Brotóns Á, Ruiz-Granell R. Identification of cavotricuspid isthmus voltage patterns in typical atrial flutter ablation. *J Arrhythmia*. 2024;40:191–194. <https://doi.org/10.1002/joa3.12982>